Indian Journal of Pure & Applied Physics
Vol. 63, January 2025, pp. 51-61
DOI: 10.56042/ijpap.v63i1.12993

Numerical Approach based Study of MHD Viscous and Viscoelastic Immiscible Fluids Flow through Porous Channel

Neeraj Srivastava* & Rajesh Johari

Department of Mathematics, Agra College, Agra, Uttar Pradesh 282 001, India

Received 7 August 2024; accepted 17 December 2024

The study and application of multiphase magnetohydrodynamic (MHD) fluid flow in porous media extend to several fields including petroleum engineering, environmental engineering, polymer processing and manufacturing, and several others. In these industries, the flow of viscous and viscoelastic fluids prevails through various channels where the many flow issues exist and require extensive investigation. In the present study, the viscous and viscoelastic immiscible magnetohydrodynamic (MHD) fluid flow through a porous horizontal channel between two plates is examined. In the channel, the viscoelastic fluid flows in upper region and the viscous fluid flows in the lower region. The flow is considered to be through a constant pressure gradient. The porous media of the upper and lower regions have two different permeabilities. The governing equations and boundary conditions are derived as per the channel geometry for these flows. These differential equations are solved analytically. The roots of the cubic equation in the viscoelastic fluid governing equation are obtained for different values of the viscoelastic parameter and permeability coefficient. The boundary conditions are applied to these solutions and obtained equations are solved numerically to obtain the values of coefficients involved in the solution using a MATLAB program. Finally, the effect of various flow governing parameters is shown on velocity profiles through various graphs. The results show that on applying the magnetic field velocity decreases. It has been shown that the MHD field application causes a drop in shear stress at the lower plate while increasing in the upper plate. The magnetic field effect on volume flow rate is also analysed and found that it increases with increasing magnetic field values. The effect of other parameters is also shown on shear stress and flow rate and the results are discussed through various graphs and tables.

Keywords: Viscosity; Viscoelasticity; MHD; Fluid dynamics; Shearing stress

1 Introduction

The behavior of fluids (liquids and gasses) in motion is the subject of fluid dynamics. Its fundamental principles and equations have numerous applications in various domains. For the design and optimization of fluid-flowing systems in engineering, such as water treatment plants, ventilation systems, and pipelines, fluid dynamics is essential. In environmental science studies, fluid dynamics is used to describe and forecast natural phenomena such as ocean currents, weather patterns, and pollution dispersion. Understanding blood flow in the cardiovascular system is vital for the diagnosis and treatment of diseases like atherosclerosis and aneurysms, and fluid dynamics is a valuable tool in medical science. In industry, fluid dynamics is used to enhance the efficiency of operations such as mixing, heating, and chemical reactions. In today's scenario almost in all aspects fluid problems can be observed in surroundings. However, modeling these problems and getting an accurate solution is a more challenging. Researchers across the domain have made significant contributions towards modeling these problems in complex equations so that they can be close to real scenarios and determine their solutions using various techniques. In practice, in most of places, two or more fluids flows are observed most often rather than a single fluid flow. If these fluids are of different viscosities or have distinct phases that cannot be mixed, they are called immiscible fluids. The modeling and solution of such fluid flow is the requirement of different industries.

These days, viscous and viscoelastic fluids that flow through various geometries are more common in industry. Many investigations are conducted regarding the flow of these fluids. The investigation on the steady and unsteady flow of incompressible viscous fluid was conducted by Kawahara *et al*. & Lalanne *et al*.[1,2]. Direct numerical simulation was performed by Canuto *et al*. to investigate compressible viscous flow around a circular cylinder[3]. Liu, Li & Lind *et al*. used the Smoothed Particle

*Corresponding author: (E-mail: msgaurineeraj@gmail.com)

Hydrodynamics (SPH) approach and talked about the latest developments and future trends in viscous incompressible flow modeling[4,5]. A three-dimensional viscous incompressible flows problem was solved using a new parallel, computationally efficient immersed technique by Liska & Colonius[6]. The issue of consistent incompressible fluid flow across curved pipes was examined by Canton *et al*.[7]. Computable flows and robust estimates for inf-sup stable FEM were used for the time-dependent incompressible Navier-Stokes equations by Schroeder *et al*.[8]. Peshkov discussed about a hyperbolic model as an alternative to the Navier-Stokes equations for viscous Newtonian flows[9]. The governing equations of motion for a viscous incompressible material surface were determined by Jankuhn *et al*.[10].

Researchers also study viscoelastic fluid flow problems through different channels using different methodologies. The resonance phenomena in viscoelastic fluid laminar flow via a pipe were studied by Letelier *et al*.[11]. In their experiment, Ibezim *et al*. investigated the relationship between the fluid viscoelasticity and the micro-porous structure through their experiment for the flexible polymer flow solutions through a unique micro-porous structure[12]. Viscoelastic fluid flow across a three-dimensional random porous medium was simulated by De *et al*.[13]. The unsteady boundary layer natural convection heat transfer of a Maxwell viscoelastic fluid over a vertical plate was investigated by Zhao *et al*.[14]. The impact of elasticity on the flow of a viscoelastic fluid via a porous pipe was investigated by Barik *et al*.[15]. The non-linear interaction between the moving viscoelastic structure and the steady laminar flow through a cylinder has been demonstrated by Mishra *et al*.[16]. The universality of coherent structures in the transition to turbulence via self-organized cycling in linearly stable plane shear flows of both elastic and Newtonian fluids was observed by Jha and Steinberg during their investigation of flow structures and properties of elastic turbulence in viscoelastic fluid flow through straight 2D channels[17]. Badami *et al*. examined the laminar fluid hammer phenomenon in viscoelastic fluids through a straight axisymmetric pipe using the finite volume approach[18]. The microscale parametric effects of viscoelastic fluid pulsating laminar flow (VPL flow) on heat transport have been reported by Zhan *et al*.[19]. In their study of the steady flow of MHD Maxwell viscoelastic fluid on a flat porous plate, Sudarmozhi *et al*. discovered an inverse relationship between the Eckert and Nusselt numbers[20].

Magnetohydrodynamics (MHD) is the study of how a magnetic field affects fluid flow in fluid dynamics. It significantly impacts how electrically conductive fluids behave. Many researchers examine the impact of MHD on fluid flow. The MHD effect across a moving plate in a rotating fluid with free stream velocity was investigated by Takhar *et al*.[21]. Turkyilmazoglu investigated the heat transfer and MHD fluid flow caused by a revolving disk that is stretching[22]. Free convective heat and mass transfer for MHD fluid flow over a permeable vertical stretching sheet in the presence of radiation and buoyancy influences was studied by Rashidi *et al*.[23]. Mittal used HAM to analyze the water-based composite MHD fluid flow[24]. The MHD fluid flows across an unsteady stretched sheet with thermal radiation, changing fluid properties, and heat flux was modeled by Megahed[25]. Variable viscosity's impact on MHD viscoelastic fluid flow and heat transmission across a stretching sheet was investigated by Prasad *et al*. The impact of nonlinear radiation on entropy-optimized MHD fluid flow was examined by Kataria *et al*.[26].

Because immiscible fluid flow problems are becoming more practical and challenging, researchers have also concentrated on them. The front-tracking/ immersed-boundary approach was created by Zolfaghari *et al*. to simulate the viscoelastic two-phase flow through a capillary tube that has both a smooth and a sharply-edged constriction[27]. A computational solution for the Saffman–Taylor instability of immiscible nonlinear viscoelastic–Newtonian displacement in a Hele-Shaw cell was reported by Yazdi & Norouzi[28]. To facilitate the simulation of turbulent and inertial elastoviscoplastic fluids with a large particle and droplet count, Izbassaroy created a three-dimensional numerical solution for viscoelastic and elastoviscoplastic fluids[29].Using a numerical approach, Devakar & Raje investigated the unsteady flow of two immiscible micropolar and Newtonian fluids through a horizontal channel[30]. An unsteady flow of an immiscible micropolar fluid sandwiched between Newtonian fluids through a channel was the subject of another numerical investigation conducted by Devakar *et al*.[31]. Devakar & Raje used a numerical technique to investigate the magnetohydrodynamic time-dependent model of immiscible newtonian and micropolar fluids

across a porous channel[32]. Rodriguez & Johnsen examined the characteristics of the system of equations and suggested a unique Eulerian method for numerical simulations of wave propagation in viscoelastic media[33]. Yadav & Verma talked about the flow of immiscible micropolar fluids via porous cylindrical pipes that enclose cavities, both Newtonian and non-Newtonian[34]. Two immiscible Newtonian and micropolar fluid flows over an inclined porous channel have been analyzed by Yadav & Verma[35]. In a vertical porous channel filled with a two-layered viscoelastic liquid, Devi & Srinivas examined the heat and mass characteristics as well as the impacts of chemical reactions, thermal radiation, Hall current, and heat source[36].

Fluid flow study through porous media has importance across a range of scientific, engineering, and environmental fields due to the unique characteristics of porous materials, which consist of interconnected voids that allow fluids (liquids and gases) to flow through them. Tlau & Ontela discussed the issue of entropy generated in a mixed convection Cu-water nanofluid flow in an inclined channel filled with a non-Darcy porous medium with variable permeability[37]. Further, Tlau & Ontela analysed the second law analysis of copper-water nanofluid flow in an inclined porous channel[38]. They extended their work and discussed the various fluid flow problems through porous media. Tlau & Ontela[39-41].

From the above discussion, it is evident that the MHD flow of viscous and viscoelastic fluids has wide applications in industry, environment, and medical sciences. Considering these important aspects, the present problem is formulated. This work deals with the problems of steady MHD flow of viscous and viscoelastic fluids through a porous channel. The flow is considered between two parallel plates. The flow governing continuity and momentum equations are derived for both the fluid flow as per the channel geometry. For the viscoelastic fluid flow, Walter's B liquid equations are used in this study. The differential equations are solved analytically. The non-linear equations are solved numerically using MATLAB after applying boundary conditions for fluid velocity solutions. The roots of the cubic equation involved in the governing equation of viscoelastic fluid are also found using MATLAB for different permeability and viscoelasticity coefficients. Since this flow is governed by various parameters, the effect of each parameter is shown on velocity profiles and shearing stress on both plates and volume flow rate. Results for velocity, shear stress, and volume flow rate are shown through various graphs and tables.

2 Mathematical Formulation

Figure 1 shows the two immiscible fluids flow is modelled through a horizontal porous channel which has resilient impermeable boundaries. The viscoelastic fluid is considered in upper part and viscous fluid flow in lower part of the channel. x axis is taken along the plates and y axis is taken perpendicular to plates. A transverse constant magnetic field is applied in the direction of y axis. Let u=$u(\bar{u}_1, \bar{u}_2)$ and v=$v(\bar{v}_1, \bar{v}_2)$ are the velocities of immiscible viscous and viscoelastic fluids respectively in x and y directions.

The governing equations of motions for both the viscous and viscoelastic regions are as follows[42-44]:

For viscous fluid flow region

$$\frac{D\rho_1}{Dt} = -\rho_1 \nabla . u \qquad \text{... (1)}$$

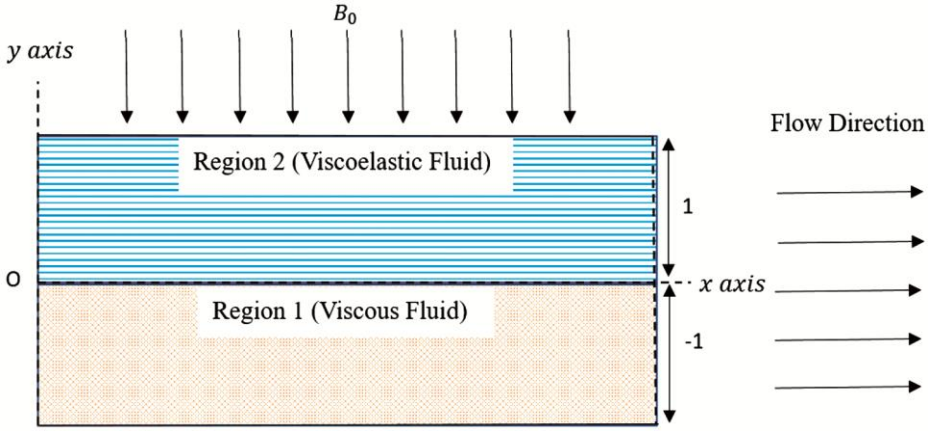

Fig. 1 — Flow of two immiscible viscous and viscoelastic fluids between two parallel plates.

$$\rho_1\left(\frac{\partial u}{\partial t}+(u.\nabla)\mathrm{u}\right)=-\nabla p_1+\mu_1\nabla^2 u-\frac{\mu_1}{K_1}u+\rho f-\sigma B_0^2 u \quad \text{... (2)}$$

For viscoelastic fluid flow region

$$\nabla.v=0 \quad \text{... (3)}$$

$$\frac{\partial v}{\partial t}+(v.\nabla)v=-\frac{1}{\rho_2}\nabla p_2+\frac{\mu_2}{k}v-\sigma B_0^2 v \quad \text{... (4)}$$

Here ρ_i, μ_i, K_1 and $K_2$are the density, viscosity, and permeability of the medium for region1 and region 2 respectively.$p_1$and p_2 are the pressure gradients applied along the flow direction in region 1 and region 2 respectively. σ is the conductivity of the fluid, B_0 is the magnetic field intensity. For the steady incompressible fluid flow under a constant pressure gradient in the absence of external forces above equations become as follows:

For region 1 the governing equations are given as

$$\frac{\partial \bar{u}_1}{\partial \bar{x}}=0 \quad \text{... (5)}$$

$$\bar{\mu}_1\frac{\partial^2 \bar{u}_1}{\partial \bar{y}^2}-\frac{\bar{\mu}_1}{\bar{K}_1}\bar{u}_1=\frac{\partial \bar{p}_1}{\partial \bar{x}}+\bar{\sigma}\bar{B}_0^2\bar{u}_1 \quad \text{... (6)}$$

For region 2 the governing equations are given as

$$\frac{\partial \bar{v}_2}{\partial \bar{y}}=0 \quad \text{... (7)}$$

which gives$\bar{v}_2=-V_0$(Constant)

$$\bar{\sigma}\bar{B}_0^2\bar{v}_1+\frac{\partial \bar{p}_2}{\partial \bar{x}}+\rho_2\bar{v}_2\frac{\partial \bar{v}_1}{\partial \bar{y}}=\bar{\mu}_2\frac{\partial^2 \bar{v}_1}{\partial \bar{y}^2}-\overline{K}\overline{v}_2\frac{\partial^3 \bar{v}_1}{\partial \bar{y}^3}-\frac{\bar{\mu}_2}{\bar{K}_2}\bar{v}_1 \quad \text{... (8)}$$

The boundary conditions are given as

$$\bar{v}_1=0:\bar{y}=h \quad \text{... (9)}$$

$$\bar{u}_1=0:\bar{y}=-h \quad \text{... (10)}$$

$$\bar{u}_1=\bar{v}_1 \text{ at } \bar{y}=0 \quad \text{... (11)}$$

The shear stress at the interface of immiscible fluids are given as

$$\tau_1=\tau_2\ i.e.\left(\frac{\partial \bar{v}_1}{\partial \bar{y}}\right)_{y=0}=\lambda\left(\frac{\partial \bar{u}_1}{\partial \bar{y}}\right)_{y=0} \quad \text{... (12)}$$

The mass conservation equation is given as[45]

$$\int_{-h}^{0}\bar{u}=Q \quad \text{... (13)}$$

Here, $Q=\bar{u}h$

3 Solution of Problem

Introducing the following non-dimensional quantities to find the solution of problem:

$$x=\frac{V_0\bar{x}}{u_2},\quad y=\frac{V_0\bar{y}}{\nu_2},\quad u_1=\frac{\bar{u}_1}{V_0},$$
$$v_1=\frac{\bar{v}_1}{V_0},\quad K_1=\frac{V_0^2\bar{K}_1}{\nu_2^2},\quad K_2=\frac{V_0^2\bar{K}_2}{\nu_2^2},$$
$$K=\frac{\bar{K}\bar{V}_0^2}{\rho_2\nu_2^2},\quad Re_1=\frac{\rho_1\nu_2^2}{\bar{\mu}_1\nu_1V_0},$$
$$Re_2=\frac{\nu_2}{u_2V_0},\quad p_1=\frac{\bar{p}_1}{\rho_1V_0},\quad p_2=\frac{\bar{p}_2}{\rho_2V_0},$$
$$\nu_2=\frac{\bar{\mu}_2}{\rho_2},\ M_1^2=\frac{\sigma\bar{B}_0^2\nu_2^2}{\bar{\mu}_1V_0^2},\ M_2^2=\frac{\sigma\bar{B}_0^2\nu_2}{V_0^2\rho_2} \quad \text{... (14)}$$

Using Eq. (14), Eqs. (5,6) & (8) becomes

$$\frac{\partial u_1}{\partial x}=0 \quad \text{... (15)}$$

$$\frac{\partial^2 u_1}{\partial y^2}-\frac{1}{K_1}u_1=Re_1\frac{\partial p_1}{\partial x}+M_1^2u_1 \quad \text{... (16)}$$

$$K\frac{\partial^3 v_1}{\partial y^3}+\frac{\partial^2 v_1}{\partial y^2}+\frac{\partial v_1}{\partial y}-\frac{1}{K_2}v_1=Re_2\frac{\partial p_2}{\partial x}+M_2^2v_1 \quad \text{... (17)}$$

The boundary conditions in non-dimensional form are given as

$$v_1=0:y=1 \quad \text{... (18)}$$

$$u_1=0:y=-1 \quad \text{... (19)}$$

$$u_1=v_1 \text{ at } y=0 \quad \text{... (20)}$$

The shear stress at the interface of immiscible fluids are given as

$$\tau_1=\tau_2\ i.e.\left(\frac{\partial v_1}{\partial y}\right)_{y=0}=\lambda\left(\frac{\partial u_1}{\partial y}\right)_{y=0} \quad \text{... (21)}$$

The mass conservation equation is given as[45]

$$\int_{-1}^{0}u=1 \quad \text{... (22)}$$

Following solution of region 1 velocity is obtained after solving equation (16)

$$u_1=C_1e^{Ay}+C_2e^{-Ay}-\frac{Re_1P_1}{A^2} \quad \text{... (23)}$$

where $A^2=\frac{1}{K_1}+M_1^2$, $C_1$and C_2 are the arbitrary constants and $Re_1$and Re_2 are the Reynolds numbers.M_1 and M_2 are the magnetic field parameters.

Equation (17) solved numerically using different values of elastic parameter K and permeability coefficient $K_2$to find the roots α,β and γ. A general solution can be written as

$$v_1=C_3e^{\alpha y}+C_4e^{\beta y}+C_5e^{\gamma y}-\frac{Re_2P_2}{B} \quad \text{... (24)}$$

where parameters α, β and γ depends on different values of viscoelasticity coefficient(K) and region 2 permeability(K_2) and $B = \frac{1}{K_2} + M_2^2$.$P_1$ and P_2 are the pressure constant for both the regions. In case of $M_1 = M_2$, the magnetic field is represented by M.

On applying boundary conditions from Eqs. (18-22), Eqs. (23 & 24) become:

$$C_1 e^{-A} - C_2 e^{A} - \frac{Re_1 P_1}{A^2} = 0 \quad \text{... (25)}$$

$$C_3 e^{\alpha} + C_4 e^{\beta} + C_5 e^{\gamma} - \frac{Re_2 P_2}{B} = 0 \quad \text{... (26)}$$

$$C_3 + C_4 + C_5 - C_1 - C_2 + \frac{Re_1 P_1}{A^2} - \frac{Re_2 P_2}{B} = 0 \quad \text{... (27)}$$

$$\lambda A C_1 - \lambda A C_2 - \alpha C_3 - \beta C_4 - \gamma C_5 = 0 \quad \text{... (28)}$$

$$\frac{C_1}{A} - \frac{C_2}{A} - \frac{C_1 e^{-A}}{A} + \frac{C_2 e^{-A}}{A} - \frac{Re_1 P_1}{A^2} - \frac{Re_2 P_2}{B} + \frac{C_3}{\alpha} + \frac{C_4}{\beta} + \frac{C_5}{\gamma} - \frac{C_3 e^{-\alpha}}{\alpha} - \frac{C_3 e^{-\beta}}{\beta} - \frac{C_3 e^{-\gamma}}{\gamma} - 1 = 0 \quad \text{... (29)}$$

4 Shear stress and total volume flow rate

The shear stress on the upper plate (τ_{upper}) and lower plates (τ_{upper}) are estimated and given as

$$\tau_{upper} = \left(\frac{\partial v_1}{\partial y}\right)_{y=1} \quad \text{... (30)}$$

$$\tau_{lower} = \lambda \left(\frac{\partial u_1}{\partial y}\right)_{y=-1} \quad \text{... (31)}$$

Using Eqs. (23 & 24) in Eqs. (30 & 31) respectively, following expressions are obtained:

$$\tau_{upper} = \alpha C_3 e^{\alpha} + \beta C_4 e^{\beta} + \gamma C_2 e^{\gamma y} \quad \text{... (32)}$$

$$\tau_{lower} = \lambda A (C_1 e^{-A} - C_2 e^{A}) \quad \text{... (33)}$$

Total volume flow rate(Q) is given as

$$Q = \int_0^1 v_1 dy + \int_{-1}^0 u_1 dy \quad \text{... (34)}$$

$$Q = \frac{C_3 e^{\alpha}}{\alpha} + \frac{C_4 e^{\beta}}{\beta} + \frac{C_5 e^{\gamma}}{\gamma} - \left(\frac{C_3}{\alpha} + \frac{C_4}{\beta} + \frac{C_5}{\gamma}\right) - \frac{Re_2 P_2}{B} + \frac{C_1 - C_2}{A} - \left(\frac{C_1 e^{-A}}{A} - \frac{C_2 e^{A}}{A} + \frac{Re_1 P_1}{A^2}\right) \quad \text{... (35)}$$

5 Results and Discussion

5.1 The effect of Magnetic field parameter (M) on parameters α, β, and γ with different viscoelasticity coefficient(K)

In Table 1, the solutions of parameters α, β, and γ for different values of M are shown. In this case same magnetic field in both the regions are taken. It can be seen from Table 1 that the values of parameter αincreases from -8.6583 to -8.0924 on increasing the magnetic field parameter from $M = 1$ to $M = 2$. In this case viscoelasticity parameter K is taken at 0.10 and other parameters remain constant. The increment is also seen for the parameter γ while the parameter β decreases from -2.1086 to -3.4731 on increasing magnetic field parameters. When the viscoelastic parameter is increased from 0.10 to 0.11, the parameter αincreases from -8.6583 to -7.6944 under the same magnetic field condition and increases further on increasing magnetic parameter values irrespective of different viscoelasticity values. This signature is just reversed for parameter β which decreases with increasing value of K and decreasing further on increasing value of M. The parameter γ follows same pattern as followed by parameter α which decreases with the increasing value of K but increases on increasing magnetic field parameter M for both the cases of viscoelasticity parameter K.

5.2 The effect of magnetic field parameter (M)on different constants and velocity profile with variable viscoelasticity coefficient(K).

Equations (16 & 17) are solved considering ordinary differential equations for u_1 and v_1 are obtained and shown in Eqs. (23 & 24). These equations involve constants C_1, C_2, C_3, C_4 and C_5 which are solved using the different boundary conditions given in Eqs. (18-22) & Eqs. (25-29) are

Table 1 — The solution of parameters α, β, and γ for different values of K and M

$K_1 = 1.5, K_2 = 2.5, P_1 = -0.7, P_2 = -0.7, Re_1 = 1.4, Re_2 = 1.6, \lambda = 0.8,$

Coefficients	Magnetic field parameter(M)					
	1		1.5		2	
	Viscoelastic Parameter(K)					
	0.10	0.11	0.10	0.11	0.10	0.20
α	-8.6583	-7.6944	-8.4441	-7.4314	-8.0924	-6.9583
β	-2.1086	-2.1617	-2.7128	-2.8123	-3.4731	-3.6904
γ	0.7668	0.7652	1.1569	1.1527	1.5655	1.5577

Table 2 — The solution of constants C_1, C_2, C_3, C_4, and C_5 for different values of M and K

$K_1 = 1.5, K_2 = 2.5, P_1 = -0.7, P_2 = -0.7, Re_1 = 1.4, Re_2 = 1.6, \lambda = 0.8$

Coefficients	Magnetic field parameter (M)					
	1		1.5		2.0	
	Viscoelasticity Coefficients (K)					
	0.10	0.11	0.10	0.11	0.10	0.11
C_1	-0.1411	-0.1418	-0.0497	-0.0509	-0.0156	-0.0170
C_2	-0.1510	-0.1510	-0.0593	-0.0592	-0.0240	-0.0240
C_3	0.0011	0.0027	0.0015	0.0039	0.0024	0.0071
C_4	-0.1417	-0.1429	-0.0656	-0.0685	-0.0336	-0.0392
C_5	-0.3636	-0.3645	-0.1315	-0.1322	-0.0530	-0.0534

obtained. The solutions of these constants for different magnetic field parameter values are given in Table 2. It is seen from the Table that on increasing the value of M, all the constants increases irrespective of any value of K. On increasing the viscoelasticity parameter, these parameters behave differently. The parameters C_1, C_4 and C_5 decreases with increasing value of K. C_2 remain almost constant in all three cases. C_3 increases with increasing value of K in all three magnetic field values.

The effect of the magnetic field parameter M is shown on the velocity parameter in Fig. 2. Magnetic fields of different intensities (1, 1.5, and 2) are applied perpendicular to the flow direction, which introduces a Lorentz force that acts against the fluid's motion. This force generates additional resistance to fluid flow which reduces the fluid velocity which is seen in the present case. Because the Lorentz force slows down the fluid near the boundary, stabilizing the boundary layer and reducing momentum transfer. The solid part of the line represents the viscous fluid velocity while the dashed line shows the velocity profile of viscoelastic fluid. The equal magnetic fields $M_1 = M_2 = M$ are applied in this case. From the figure, it can be seen that increasing the magnetic field from $M = 1$ to $M = 2$ the velocity reduces for both the fluids. The velocity is maximum at the y$= 0$ and is close to 0.3, 0.2, and 1.5 when M is 1, 1.5, and 2 respectively. The velocity reduces from y$= 0$ on both sides and becomes zero at the lower ($y = 0$) and upper plate ($y = 1$). Increasing the viscoelasticity parameter also reduces the velocity for all three magnetic field values but this decrement is much less as compared to changes due to the magnetic field parameter. This happens because Lorentz force acts opposite to the flow direction, creating a retarding or drag force on the fluid. The greater the strength of the transverse magnetic field, the larger the Lorentz force

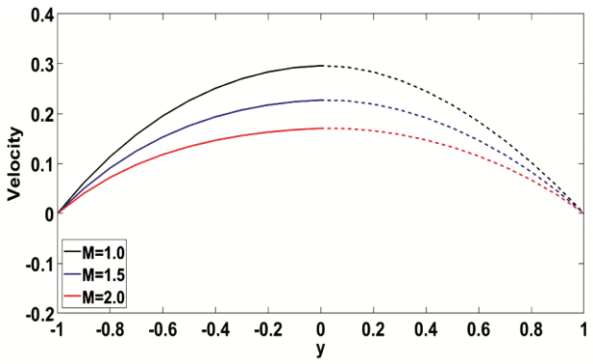

Fig. 2 — The effect of Magnetic field parameter (M) on velocity profile. u_1 - solid line, u_2 - dash line.

becomes, which increases the effective resistance to the fluid flow, thereby reducing the fluid's velocity. Similar decreasing results of velocity for increasing value of magnetic field parameter are also found in other studies[25,45,46].

5.3 The effect of magnetic field parameter (M)on different constants and velocity profile with variable viscosity ratio (λ)

The effect of magnetic field parameter (M) on C_1, C_2, C_3, C_4, and C_5 with different viscosity ratio parameters is shown through Table 3. It is seen that on increasing the values of M for $\lambda = 1$, all coefficient values increase with a minimum at $M = 1$ to maximum at $M = 2$. On increasing the viscosity ratio from $\lambda = 1$ to $\lambda = 5$, a similar effect is seen. In this case also all coefficient values increase on increasing magnetic field parameters. On comparing the coefficients value of $\lambda = 1$ and $\lambda = 5$, it is observed that C_1 and C_4 decreasing, C_3 almost remains constant and C_2 and C_5 increases with increasing viscosity ratio. Fig. 3 shows the velocity profile for $M = 1, 1.5$ and 2 in the case of $\lambda = 1$. It is seen that in this case also the velocity profile comes down on increasing the magnetic field parameter.

Table 3 — The solution of constantsC_1, C_2, C_3, C_4,and C_6 for different values of M and λ

$K_1 = 1.5, K_2 = 2.5 P_1 = -0.7, P_2 = -0.7, Re_1 = 1.4, Re_2 = 1.6, K = 0.10$

Coefficients	Magnetic field parameter(M)					
	1		1.5		2	
	Viscosity ratio coefficients (λ)					
	1	5	1	5	1	5
C_1	-0.1418	-0.1471	-0.0505	-0.0557	-0.0163	-0.0209
C_2	-0.1510	-0.1506	-0.0592	-0.0591	-0.0200	-0.0239
C_3	0.0011	0.0011	0.0015	0.0016	0.0024	0.0025
C_4	-0.1424	-0.1475	-0.0664	-0.0716	-0.0342	-0.0390
C_5	-0.3636	-0.3633	-0.1315	-0.1314	-0.0530	-0.0529

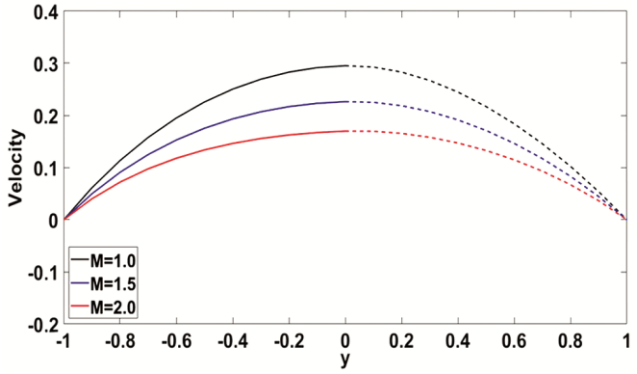

Fig. 3 — The effect of Magnetic field parameter (M) on velocity profile when$\lambda = 1$. u_1 - solid line, u_2 - dash line.

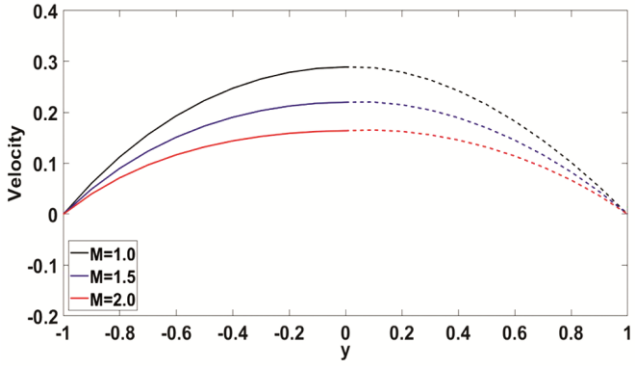

Fig. 4 — The effect of Magnetic field parameter (M) on velocity profile when$\lambda = 10$. u_1 - solid line, u_2 - dash line.

A similar effect is shown in Fig. 4 for $\lambda = 10$. On increasing the viscosity ratio, the velocity reduces further. When the viscosity ratio increases, the internal friction within the fluid increases. This friction acts to resist the motion of fluid layers relative to each other, effectively slowing down the flow velocity for constant pressure gradient. So magnetic field parameter and viscoelasticity ratio both reduce the velocity. The maximum velocity close to 0.3 is seen at $y = 0$ in this case also for $M = 1$.

5.4 The effect of magnetic field parameter(M)on different constants velocity profiles with different permeability parameters K_1 and K_2.

In Table 4 the effect of permeability parameters $K_1$and K_2 and magnetic field parameter $M$are shown on constants. It is found that C_1 and C_2 are decreasing, C_2 remains constant while C_4 and C_5 increase with same magnetic field parameter M, considering all three cases of permeabilities. On comparing the coefficients with different permeability conditions under different magnetic field cases, it is observed that on increasing the magnetic field parameter the values of C_1, C_2, C_3, C_4, and C_5 increase in all three cases of permeability conditions.

Figures 5-7 show the velocity profiles under different magnetic field conditions of $K_1 < K_2$, $K_2 > K_1$ and $K_1 = K_2$ respectively. In this case also on increasing the magnetic field parameter, velocity decreases. The peak velocity is observed at $y = 0$ and reaches zero near to plate. In case of $K_1 = K_2$ the velocity at $y = 0$ is 0.3 and it reduces in case of $K_2 < K_1$ and reduces further when $K_2 > K_1$. This shows that if the permeability of both mediums is equal then the velocity at $y = 0$ will be maximum but if both the permeabilities are not equal the maximum velocity will reduce. It is also observed that increasing the permeability of a porous medium increases the fluid velocity because it reduces the resistance within the medium and allows fluid to flow with fewer obstructions and at a greater velocity for a given pressure gradient.

5.5 The effect of different magnetic field parameter M_1 and M_2 on velocity profiles

Figure 8 represents the velocity profile in case of different intensity magnetic fields M_1 and $M_2$are applied in region 1 and region 2 respectively. It is seen that velocity decreases on increasing M_1 in the region 1. All the velocity profiles meet closely at a point between -0.2 and 0 in region 1 and after that, the

Table 4 — The solution of constants C_1, C_2, C_3, C_4, C_5, and C_6 for different values of M, K_1 and K_2 $P_1 = -0.7, P_2 = -0.7, Re_1 = 1.4, Re_2 = 1.6, K = 0.1, \lambda = 0.8$

Coefficients	Permeability								
	$K_1 = 1.5, K_2 = 2.5$			$K_1 = 2, K_2 = 2$			$K_1 = 2.5, K_2 = 1.5$		
	$M = 1$	$M = 1.5$	$M = 2$	$M = 1$	$M = 1.5$	$M = 2$	$M = 1$	$M = 1.5$	$M = 2$
C_1	-0.1411	-0.0497	-0.0156	-0.1813	-0.0640	-0.0218	-0.2148	-0.0763	-0.0274
C_2	-0.1510	-0.0593	-0.0240	-0.1763	-0.0656	-0.0258	-0.1943	-0.0697	-0.0269
C_3	0.0011	0.0015	0.0024	0.0011	0.0015	0.0024	0.0011	0.0015	0.0024
C_4	-0.1417	-0.0656	-0.0336	-0.1240	-0.0584	-0.0303	-0.1027	-0.0499	-0.0266
C_5	-0.3636	-0.1315	-0.0530	-0.3280	-0.1236	-0.0508	-0.2794	-0.1117	-0.0474

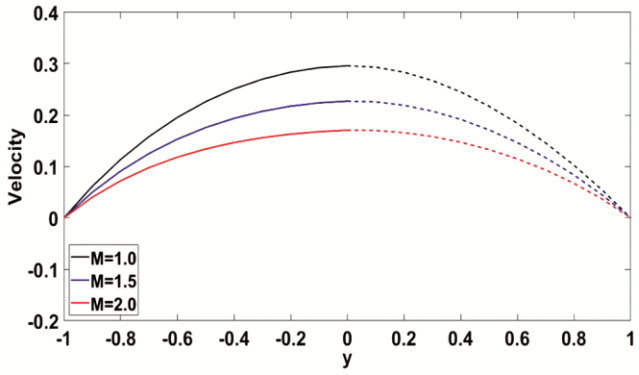

Fig. 5 — The effect of Magnetic field parameter (M)on velocity profileswhen $K_1 = 1.5$ and $K_2 = 2.5$.u_1 - solid line, u_2 - dash line.

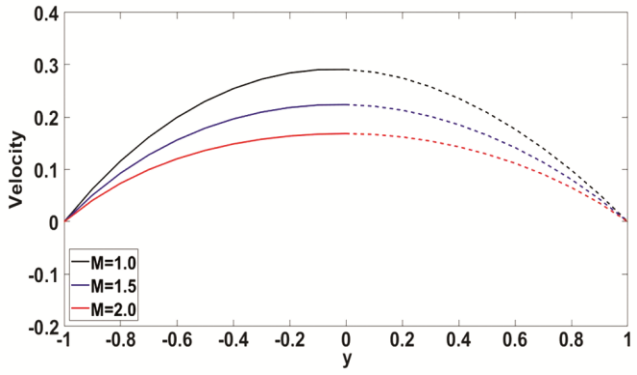

Fig. 6 — The effect of Magnetic field parameter (M) on velocity profiles when $K_1 = 2.5$ and $K_2 = 1.5$. u_1 - solid line, u_2 - dash line.

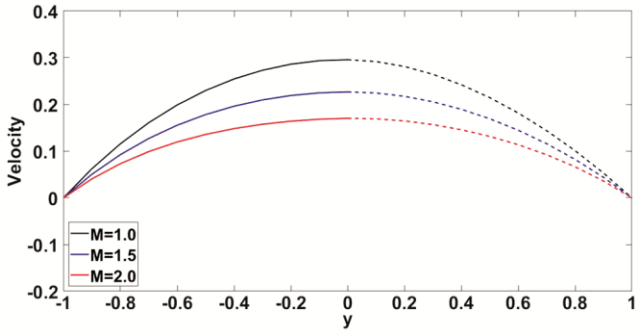

Fig. 7 — The effect of Magnetic field parameter (M) on velocity profile when $K_1 = 2.0$ and $K_2 = 2.0$. u_1 - solid line, u_2 - dash line.

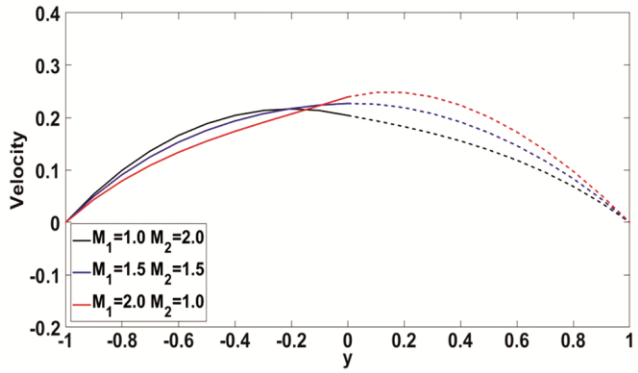

Fig. 8 — The effect of Magnetic field parameters$M_1$and M_2 on velocity profile when$K = 0.1$. u_1 - solid line, u_2 - dash line.

velocities are reversed. This means the velocity with higher M_1 value in region 1 becomes more and velocity with lower M_1 value comes downafter this point. This phenomenon is observed because of the influence of the magnetic field of region 2. The region 2 magnetic field M_2 is decreased from $M_2 = 2.0$ to $M_1 = 1.0$ in reverse order after the point $y = 0$. So reverse profiles of velocities are observed. A sensitivity analysis is also done by changing K values and observing similar results. That means for different values of K the fluid velocities pattern will remain the same. Magnetic field of both regions meets close to $y = -0.2$.

Figures 9 & 10 show the velocity profiles for $M_1 < M_2, M_1 = M_2$ and $M_1 > M_2$. The velocity profiles have been shown for different viscosity ratio parameter λ. In the figure where $\lambda = 1$, the velocity comes down as M_1 increases and M_2 decreases in region 1. Like Fig. 8, after $y = -0.2$, the magnetic field M_2 start influencing region 1 velocities, and

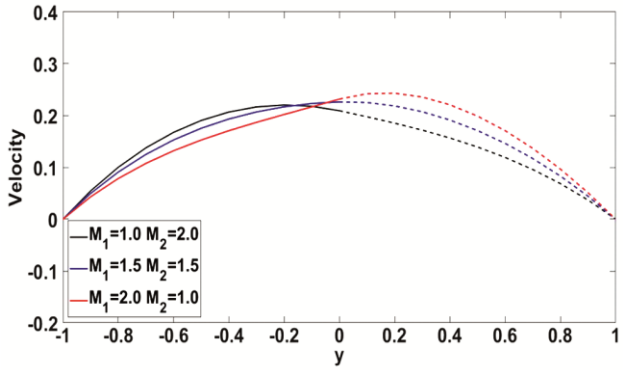

Fig. 9 — The effect of Magnetic field parameters $M_1$and M_2on velocity profile when$\lambda = 1$. u_1 - solid line, u_2 - dash line.

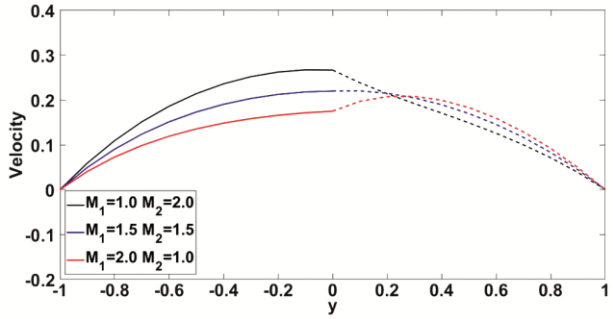

Fig. 10 — The effect of Magnetic field parameters $M_1$and M_2 on velocity profile when $\lambda = 10$. u_1 - solid line, u_2 - dash line.

because of that the velocities are reverse as the M_2 comes down from $M_2 = 2$ to $M_2 = 1$. On increasing the viscosity ratio value from $\lambda = 1$ to $\lambda = 10$ the effect of the magnetic field parameter is shown in Fig. 10. It can be seen that till $y = 0$, the velocity of region 1 reduces as the magnetic field parameter increases. The effect of region 1 magnetic field is also seen up to $y = 0.2$ in region 2. The velocities upto this point follows the same pattern as in region 1. After this point region 2 magnetic field influences and velocities order becomes reverse.

Figure 11 shows the effect of the magnetic field is also assessed with respect to different permeability conditions. It is observed that in region 1 the velocity follows the same pattern as it was in previous cases. The region 2 magnetic field influences till $y = -0.2$ in the region 1 and after that it follows the reverse pattern in region 2 where the velocity decreases on increasing the magnetic field. The point close to $y = -0.2$ is considered the point where both the magnetic field meets in this case.

5.6 Shearing stress and volume flow rate estimation

The effect of the magnetic field on shearing stress is assessed and shown in Tables 5-7. Form the Table 5

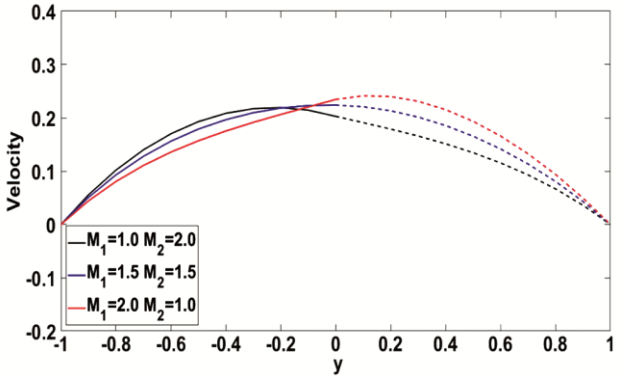

Fig. 11 — The effect of Magnetic field parameters $M_1$and M_2on velocity profile when of $K_1 = 2.5$ and $K_2 = 1.5$. u_1 - solid line, u_2 - dash line.

it can be analysed that on increasing the value of M shearing stress is increased on an upper plate while it is reduced on the lower plate because Lorentz force creates a retarding effect on the moving fluid near to upper plate, slowing down the flow and generating a velocity gradient between fluid layers, which results in an increase in shear stress. This is happening in all three cases $K_1 > K_2$, $K_1 = K_2$ and $K_1 < K_2$ of permeability. In this case, viscoelastic coefficient K is taken at 0.10. Similar trends are observed when K is increased from $K = 0.10$ to $K = 0.11$ as shown in Table 6.In this case, also, an increment in the magnetic field reduces shearing stress on the lower plate and increases on the upper plate. On comparing Table 5 & 6, it is observed that on increasing the viscoelasticity the shearing stress on the upper plate further increased and it decreased on the lower plate. In Tables 5 & 6, the viscosity ratio is taken to 0.8 which is increased to 1.0 in Table 7 to observe the magnetic field effect in case of an increment in viscosity ratio. It is observed that on increasing the magnetic field, shearing stress follows the same pattern as followed in Table 5 & 6. However, on comparing the results of Table 6 & 7, it is seen that on increasing the viscosity ratio the shearing stress decreases on the upper plate and increases on the lower plate.

5.7 The estimation of volume flow rate

Volume flow rate results are presented in Tables 8 & 9 for different cases of viscosity ratio and viscoelasticity respectively to observe the magnetic field effects. The results show that on increasing the value of M flow rate increases as seen in Table 8. On increasing the value of λ the flow rate is constant for $M = 1$ and for $M = 2$ it is increased when $K_1 > K_2$.

Table 5 — The effect of Mon shearing stress τ_{upper} and τ_{lower} ($\lambda = 0.8, K = 0.10$)

$P_1 = -0.7, P_2 = -0.7, Re_1 = 1.4, Re_2 = 1.6, \lambda = 0.8, K = 0.10$

Magnetic Field Parameter	Permeability					
	$K_1 = 2.5, K_2 = 1.5$		$K_1 = 2, K_2 = 2$		$K_1 = 1.5, K_2 = 2.5$	
	τ_{upper}	τ_{lower}	τ_{upper}	τ_{lower}	τ_{upper}	τ_{lower}
$M = 1.0$	-0.5450	0.5381	-0.5573	0.5357	-0.5640	0.5271
$M = 1.5$	-0.4592	0.4426	-0.4674	0.4404	-0.4721	0.4344
$M = 2.0$	-0.3848	0.3625	-0.3901	0.3607	-0.3933	0.3567

Table 6 — The effect of Mon shearing stress τ_{upper} and τ_{lower} ($\lambda = 0.8, K = 0.11$)

$P_1 = -0.7, P_2 = -0.7, Re_1 = 1.4, Re_2 = 1.6, \lambda = 0.8, K = 0.11$

Magnetic Field Parameter	Permeability					
	$K_1 = 2.5, K_2 = 1.5$		$K_1 = 2.0, K_2 = 2.0$		$K_1 = 1.5, K_2 = 2.5$	
	τ_{upper}	τ_{lower}	τ_{upper}	τ_{lower}	τ_{upper}	τ_{lower}
$M = 1.0$	-0.5435	0.5365	-0.5564	0.5343	-0.5635	0.5258
$M = 1.5$	-0.4559	0.4409	-0.4644	0.4388	-0.4693	0.4329
$M = 2.0$	-0.3807	0.3610	-0.3861	0.3593	-0.3894	0.3553

Table 7 — The effect of Mon shearing stress τ_{upper} and τ_{lower} ($\lambda = 1.0, K = 0.10$)

$P_1 = -0.7, P_2 = -0.7, Re_1 = 1.4, Re_2 = 1.6, \lambda = 1.0, K = 0.10$

Magnetic Field Parameter	Permeability					
	$K_1 = 2.5, K_2 = 1.5$		$K_1 = 2.0, K_2 = 2.0$		$K_1 = 1.5, K_2 = 2.5$	
	τ_{upper}	τ_{lower}	τ_{upper}	τ_{lower}	τ_{upper}	τ_{lower}
$M = 1.0$	-0.5454	0.6736	-0.5575	0.6699	-0.5638	0.6584
$M = 1.5$	-0.4593	0.5536	-0.4674	0.5505	-0.4719	0.5426
$M = 2.0$	-0.3848	0.4531	-0.3901	0.4507	-0.3932	0.4455

Table 8 — The volume flow rate for different permeability coefficients and different values of λ.

$P_1 = -0.7, P_2 = -0.7, Re_1 = 1.4, Re_2 = 1.6, K = 0.10$

Viscosity Ratio	Permeability					
	$K_1 = 2.5, K_2 = 1.5$		$K_1 = 2, K_2 = 2$		$K_1 = 1.5, K_2 = 2.5$	
	Magnetic Field Parameter (M)					
	1	2	1	2	1	2
$\lambda = 0.4$	1.3956	1.6741	1.8880	2.2276	2.3962	2.7822
$\lambda = 0.6$	1.3956	1.6741	1.8884	2.2273	2.3954	2.7817
$\lambda = 0.8$	1.3956	1.6741	1.8887	2.2271	2.3948	2.7812

Table 9 — The effect of Monvolume flow rate for different viscoelasticity coefficients.

$P_1 = -0.7, P_2 = -0.7, Re_1 = 1.4, Re_2 = 1.6, \lambda = 0.8$

Viscoelasticity	Permeability					
	$K_1 = 2.5, K_2 = 1.5$		$K_1 = 2, K_2 = 2$		$K_1 = 1.5, K_2 = 2.5$	
	Magnetic Field Parameter (M)					
	1	2	1	2	1	2
$K = 0.08$	1.3981	1.6752	1.8882	2.2280	2.3940	2.7820
$K = 0.09$	1.3984	1.6749	1.8887	2.2277	2.3946	2.7818
$K = 0.10$	1.3983	1.6741	1.8887	2.2271	2.3948	2.7812

In case of $K_1 = K_2$, the flow rate increases for $M = 1$ and decreased for $M = 2$ on increasing the viscosity ratio. When $K_1 < K_2$, the flow rate decreases for $M = 1$ and $M = 2$ as presented in Table 9. In similar way, the effect of magnetic field with increasing value of $K$is observed in Table 9. On increasing the magnetic field value the flow rate increased in all three cases of K_1 and K_2. When the

value of $K$is increased from 0.08 to 0.10, the flow rate is increased for $M = 1$ and decreased for $M = 2$ and for $K_1 = K_2$, and $K_1 < K_2$. For $K_1 > K_2$, the flow rate is increased first and decreased when $M = 1$ and it is decreased when $M = 2$.

6 Conclusion

This study investigates the flow of MHD immiscible fluids between two parallel plates. In two regions between two parallel plates, viscous and viscoelastic fluid flows are considered. A magnetic field is also applied to observe the effect on velocity profiles, shearing stress, and flow rate. Accordingly, the equations of motion for both regions are modeled and solved numerically. Magnetic field effects on shearing stress and flow rate are observed for different viscoelasticity, viscosity ratio, and permeability conditions. The major findings of the study are as follows:

- It is found that the MHD effect reduces the velocity in both regions.
- It is also observed that velocity decreases with increasing the viscoelasticity and viscosity ratio.
- It is observed that shearing stress increases on the upper plate and decreases on the lower plate after applying a magnetic field.

The results of the present analysis are very useful in polymer, food, and petroleum industries wherever MHD flow of viscous and viscoelastic fluid flow is in process.

Acknowledgements

I thank HoD, Department of Mathematics, Principal, Agra College Agra for providing research facilities to carry out this work.

Authors Contribution

Neeraj Srivastava carried out analysis and written manuscript. Rajesh Johari has provided project management support.

References

1 Kawahara M, Yoshimura N, Nakagawa K & Ohsaka H, *Int J Numer Methods Eng*, 10 (1976) 437.
2 Lalanne B, Villegas L R, Tanguy S & Risso F, *J Comput Phys*, 301 (2015) 289.
3 Canuto D & Taira K, *J Fluid Mech*, 785 (2015) 349.
4 Liu M B & Li S M, *J Hydrodyn*, 28 (2016) 731.
5 Lind S J, Stansby P K & Rogers B D, *J Comput Phys*, 309 (2016) 129.
6 Liska S & Colonius T, *J Comput Phys*, 331 (2017) 257.
7 Canton J, Örlü R & Schlatter P, *Int J Heat Fluid Flow*, 66 (2017) 95.
8 Schroeder P W, Lehrenfeld C, Linke A & Lube G, *SeMA J*, 75 (2018) 629.
9 Peshkov I & Romenski E, *Continuum Mech Thermodyn*, 28 (2016) 85.
10 Jankuhn T, Olshanskii M A & Reusken A, *Interfaces Free Boundaries*, 20 (2018) 353.
11 Letelier M F, Siginer D A, Almendra D L & Stockle J S, *Int J Non-Linear Mech*, 115 (2019) 53.
12 Ibezim V C, Poole R J & Dennis D J, *J Non-Newtonian Fluid Mech*, 296 (2021) 104638.
13 De S, Kuipers J A M, Peters E A J F & Padding J T, *J Non-Newtonian Fluid Mech*, 248 (2017) 50.
14 Zhao J, Zheng L, Zhang X & Liu F, *Int J Heat Mass Transfer*, 97 (2016) 760.
15 Barik R N, Dash G C & Rath P K, *Alexandria Eng J*, 57 (2018) 973.
16 Mishra R, Kulkarni S S, Bhardwaj R & Thompson M C, *J Fluids Struct*, 87 (2019) 284.
17 Jha N K & Steinberg V, *arXiv preprint arXiv:2009*, 12258 (2020).
18 Badami M M, Riasi A & Sadeghy K, *J Braz Soc Mech Sci Eng*, 43 (2021) 1.
19 Zhan Z, Chen L, Zhang H, Lin C, Li S, Li X & Li F, *Appl Therm Eng*, 213 (2022) 118734.
20 Sudarmozhi K, Iranian D & Khan I, *Front Phys*, 11 (2023) 1126662.
21 Takhar H S, Chamkha A J & Nath G, *Int J Eng Sci*, 40 (2002) 1511.
22 Turkyilmazoglu M, *Int J Mech Sci.*, 77 (2013) 263.
23 Rashidi M M, Rostami B, Freidoonimehr N & Abbasbandy S, *Ain Shams Eng J*, 5 (2014) 901.
24 Mittal A S, *Int J Ambient Energy*, 42 (2021) 1538.
25 Megahed A M, Reddy M G & Abbas W, *Math Comput Simul*, 185 (2021) 583.
26 Kataria H, Mittal A S & Mistry M, *Int J Ambient Energy*, 43 (2022) 6909.
27 Zolfaghari H, Izbassarov D & Muradoglu M, *Comput Fluids*, 156 (2017) 548.
28 Yazdi A A & Norouzi M, *Rheol Acta*, 57 (2018) 575.
29 Izbassarov D, Rosti M E, Ardekani M N, Sarabian M, Hormozi S, Brandt L & Tammisola O, *Int J Numer Methods Fluids*, 88 (2018) 521.
30 Devakar M & Raje A, *Eur Phys J Plus*, 133 (2018) 180.
31 Devakar M, Raje A & Kumar S, *J Appl Mech Tech Phys*, 59 (2018) 980.
32 Devakar M & Raje A, *J Appl Fluid Mech*, 12 (2019) 603.
33 Rodriguez M & Johnsen E, *J Comput Phys*, 379 (2019) 70.
34 Yadav P K & Verma A K, *Eur Phys J Plus*, 135 (2020) 645.
35 Yadav P K & Verma A K, *Math Methods Appl Sci*, 45 (2022) 1700.
36 Devi M P & Srinivas S, *Int Commun Heat Mass Transfer*, 142 (2023) 106612.
37 Tlau L & Ontela S, *Ind J Phys*, 95 (2021) 2095.
38 Tlau L & Ontela S, *Pramana*, 95 (2021) 188.
39 Tlau L & Ontela S, *Ind J Phys*, 96 (2022) 1127-1140.
40 Tlau L & Ontela S, *Chin J Phys*, 80 (2022) 239.
41 Tlau L & Ontela S, *Heat Transf*, 49 (2022) 1035.
42 Yadav P K, Jaiswal S & Sharma B D, *Appl Math Mech*, 39 (2018) 993.
43 Gaur P K & Jha A K, *Open J Fluid Dyn*, 6 (2016) 11.
44 Mahabaleshwar U S, Sarris I E & Lorenzini G, *Int J Heat Mass Transfer*, 127 (2018) 1327.
45 Sivaraj R, Kumar B R & Prakash J, *Appl Appl Math*, 7 (2012) 6.
46 Ansari I A & Deo S, *Nat Acad Sci Lett*, 40 (2017) 211.